Supplemental information:

Epigenetic regulation of starvation-induced autophagy in *Drosophila* by histone methyltransferase G9a

Phan Nguyen Thuy An[1,*], Kouhei Shimaji [2,3,*], Ryo Tanaka [2,3], Hideki Yoshida[2,3], Hiroshi Kimura[4], Eiichiro Fukusaki[1,], Masamitsu Yamaguchi[2,3,**]**

[1] Department of Biotechnology, Graduate School of Engineering, Osaka University, 2-1 Yamadaoka, Suita, Osaka, 565-0871, Japan.

[2] Department of Applied Biology, [3] The Center for Advanced Insect Research Promotion, Kyoto Institute of Technology, Kyoto, 606-8585, Japan.

[4]Departmetnt of Biological Sciences, Graduate School of Bioscience and Biotechnology, Tokyo Institute of Technology, Nagatsuta, Midori-ku, Yokohama, 226-8501, Japan.

* These authors contributed equally to this work

**Corresponding author

MY: Tel.: +81 75 724 7781; Fax: +81 75 724 7799; E-mail: myamaguc@kit.ac.jp

EF: Tel./ Fax: +81-6-6879-7424; E-mail: fukusaki@bio.eng.osaka-u.ac.jp

Table S1. Potential metabolites affected due to the loss of *dG9a* during starvation.

Compound	OPLS-DA		*p-value* from Two-way ANOVA		
	p(corr)	VIP	Starved time	Genotype	Interaction
Threonine	-0.63	1.53	7.15E-04	2.45E-07	5.40E-03
Inositol	-0.96	2.32	1.59E-05	6.88E-23	7.05E-03
Serine	0.56	1.32	1.23E-03	7.14E-06	7.05E-03
Methionine	0.65	1.61	4.65E-02	1.02E-06	7.54E-03
Uric acid	-0.92	2.26	9.71E-07	2.42E-20	3.73E-02
Tryptophan	-0.86	2.11	5.85E-06	3.43E-15	4.02E-02
Lactic acid	0.42	1.06	1.21E-02	1.62E-03	4.35E-02
Acetyl CoA	-0.54	1.34	1.51E-02	1.08E-04	0.09
Fructose	-0.53	1.21	2.39E-06	7.14E-06	0.08
Guanosine	-0.97	2.36	0.12	1.01E-20	0.20
Glutamine	0.73	1.72	4.48E-02	1.02E-06	0.21
FMN	-0.68	1.68	0.35	4.75E-06	0.23
Urea	-0.50	1.22	3.94E-02	1.62E-03	0.22
NADP	-0.49	1.20	0.19	2.77E-03	0.32
Xylitol	-0.47	1.14	0.15	5.22E-03	0.38
NADPH	0.85	2.08	0.06	1.01E-10	0.41
Ru5P	-0.48	1.14	8.52E-07	1.59E-05	0.55
cAMP	-0.41	1.01	0.13	1.03E-02	0.52
Hypoxanthine	-0.56	1.36	1.52E-02	2.35E-04	0.56
Pyruvate	0.47	1.11	1.24E-02	5.23E-03	0.56
GMP	0.62	1.43	1.31E-02	7.98E-05	0.62
Asparagine	0.63	1.52	4.70E-06	1.14E-06	0.91
G6P	-0.46	1.10	9.09E-03	2.77E-03	0.91
Inosine	-0.86	2.07	1.57E-02	9.41E-11	0.92
Malic acid	-0.49	1.22	0.18	5.35E-03	0.97

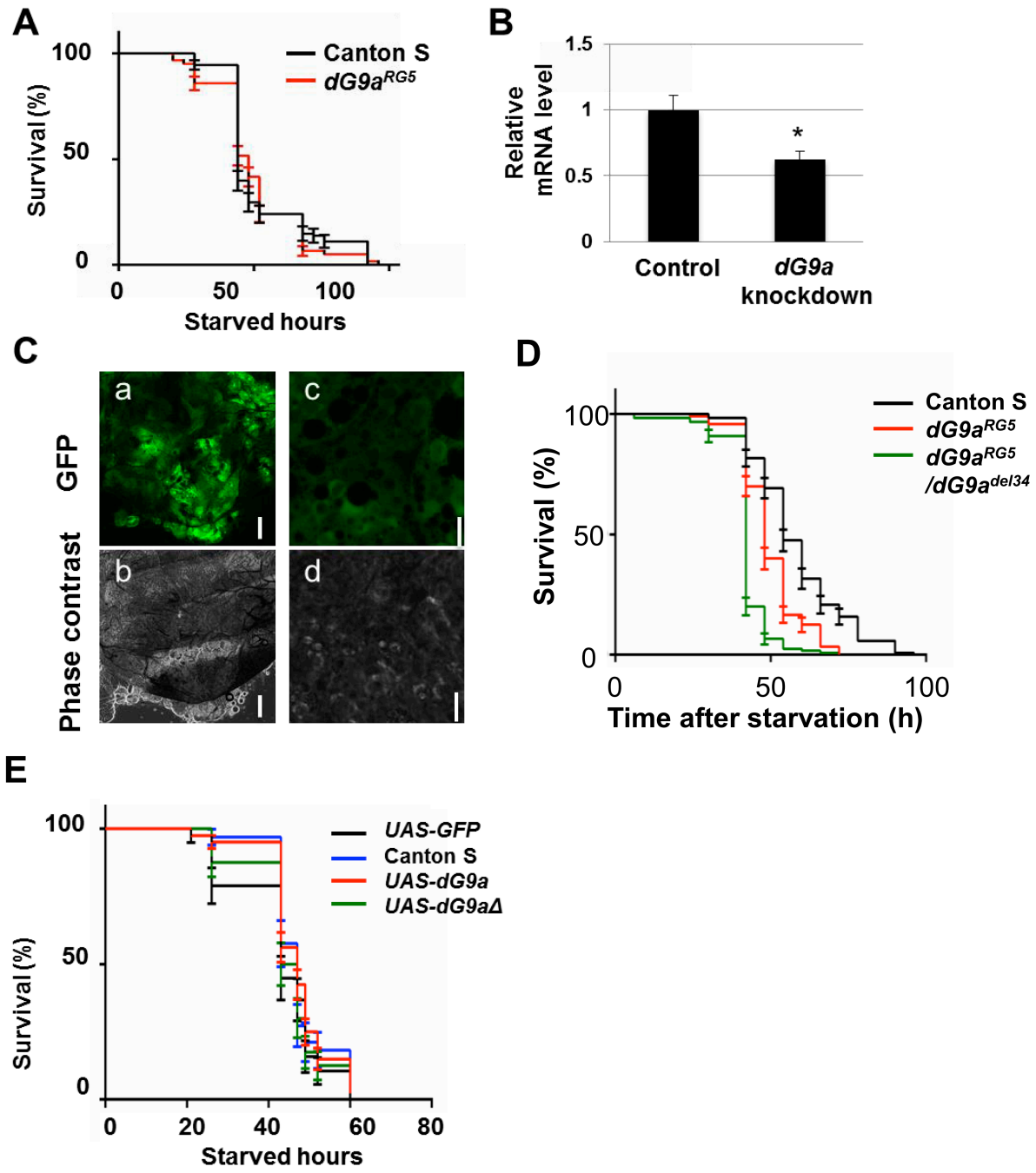

Figure S1. (A) The result of viability assay under starvation conditions using larvae of wild type and *dG9a*^{RG5} mutant (n=120 from 6 independent experiments). *P* >0.05. **(B)** Quantification of mRNA level of dG9a in fat-body specifically dG9a knockdown strain (w; FB-GAL4/UAS-FLAG-IR dG9a ;+) and control strain (w; FB-GAL4/+;+). n=3. *P<0.05. **(C)** Immunostaining with anti-GFP antibody in the adult abdominal fat body. The used fly

strain was *P(GAL4)fat; UAS-GFP*. Scale bars: (a,b) 0.9 mm, (c,d) 100µm. **(D)** The result of viability assay under starvation conditions using adult female of Canton S, $dG9a^{RG5}$ and $dG9a^{RG5}$/ $dG9a^{del34}$. n=100 from 5 independent experiments. Error bars represent standard errors (SE). Significant differences were observed between Canton S and $dG9a^{RG5}$ ($P < 0.0001$), between Canton S and $dG9a^{RG5}$/ $dG9a^{del34}$ ($P < 0.0001$) and between $dG9a^{RG5}$ and $dG9a^{RG5}$/ $dG9a^{del34}$ ($P < 0.0001$). $dG9a^{RG5}$ lacks the whole open reading frame (ORF) of *dG9a,* however, $dG9a^{del34}$ lacks a part of *CG3038* including its transcription start site as well as almost all of the ORF of *dG9a* [21]*. CG3038* is suggested to have glycosyl transferase activity based on the sequence and structural similarity (Flybase:http://flybase.org/). The possible reduction of *CG3038* may result in the further reduction of starvation tolerance in $dG9a^{RG5}$/ $dG9a^{del34}$ compared with $dG9a^{RG5}$ flies. **(E)** The results of viability assay under starvation conditions utilizing male flies of *UAS-GFP* (*UAS-GFP/*+) (n=38 from 2 independent experiments), Canton S (n=33 from 2 independent experiments), *UAS-dG9aΔ* (*UAS-dG9aΔ/*+) (n=40 from 2 independent experiments) and *UAS-dG9a* (*UAS-dG9a/*+) (n=80 from 4 independent experiments). $P > 0.05$.

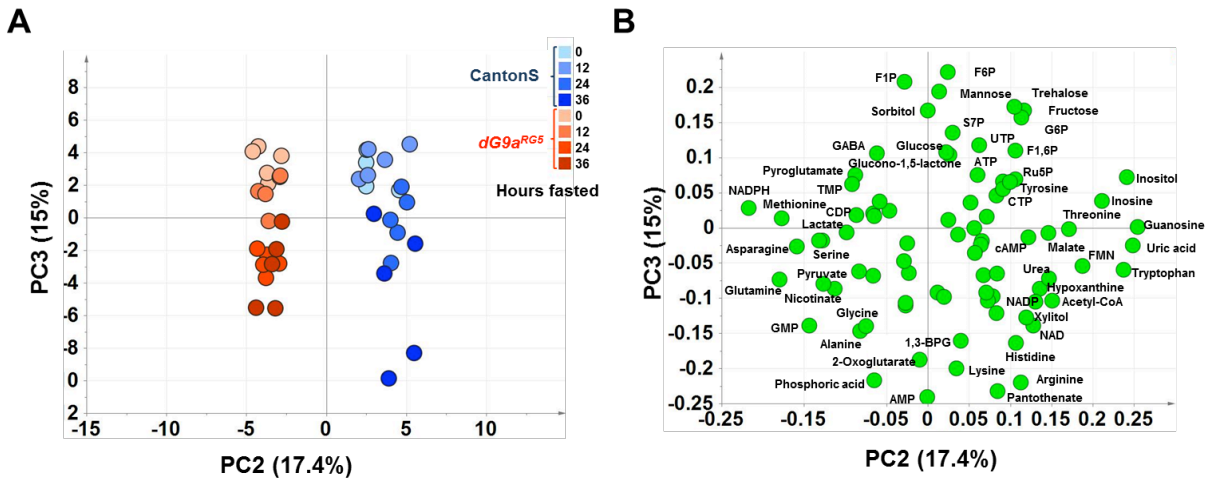

Figure S2. Metabolic profile of wild type and *dG9a*^{RG5} mutant flies under starvation. PCA score plot (upper panel) constructed by PC2 (17.4%) and PC3 (15%) shows the discriminations in genotypes and in various time points under starvation. This discrimination is explained by the composition of metabolites on loading plot (lower panel). 4-5 replications for each time point.

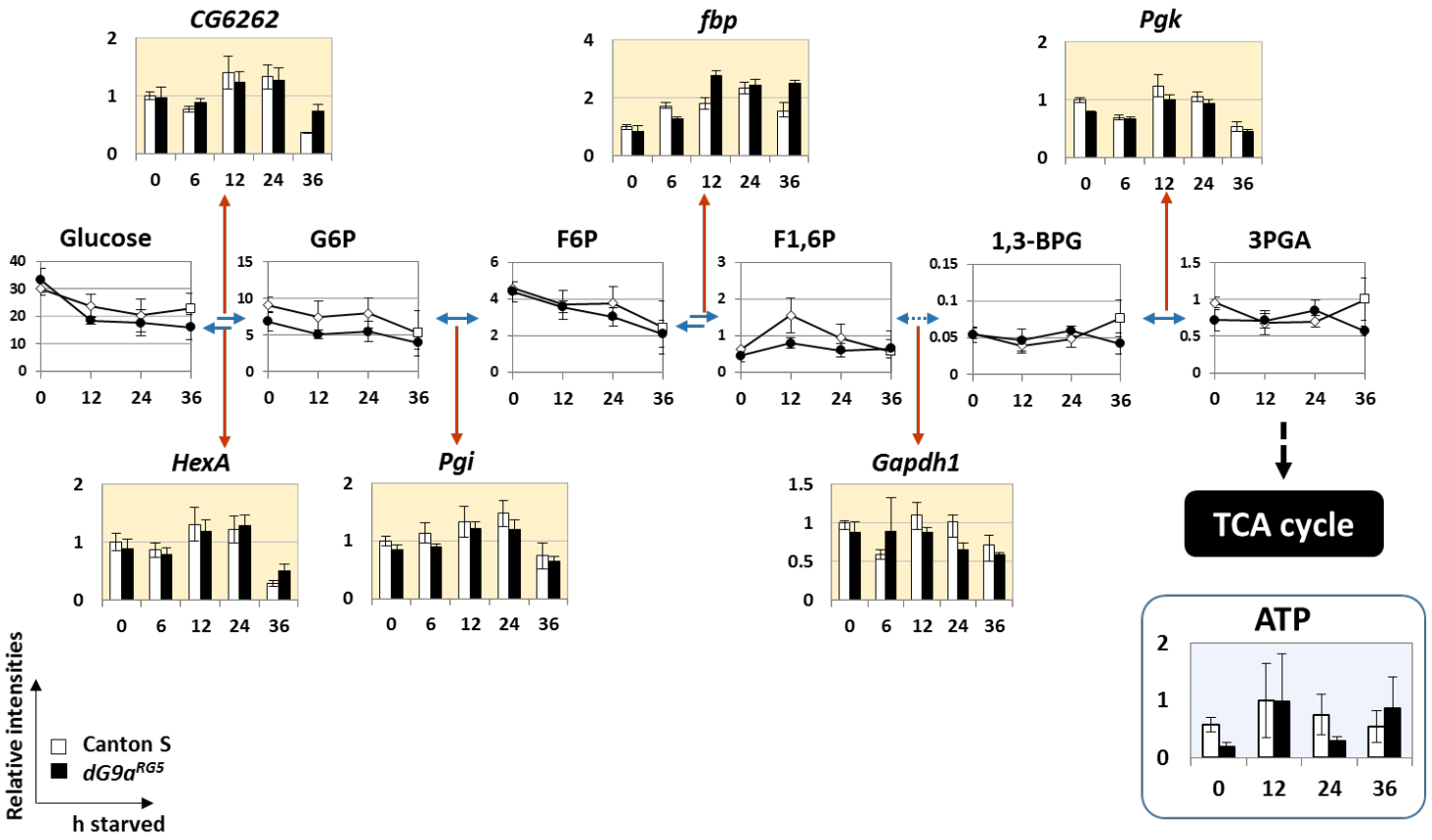

Figure S3. Glycolysis pathway of wild type and *dG9a*^{RG5} mutant flies during fasting. The line graphs showing the changes of metabolites. 4-5 replications for each time point. The bar graphs showing the mRNA level of enzymes related to glycolysis. 1,3-BPG: 1,3-Biphosphoglycerate; 3PGA: 3-Phosphoglycerate; F6P: Fructose 6-phosphate; F1,6P: Fructose 1,6-phosphate; G6P: Glucose 6-phosphate

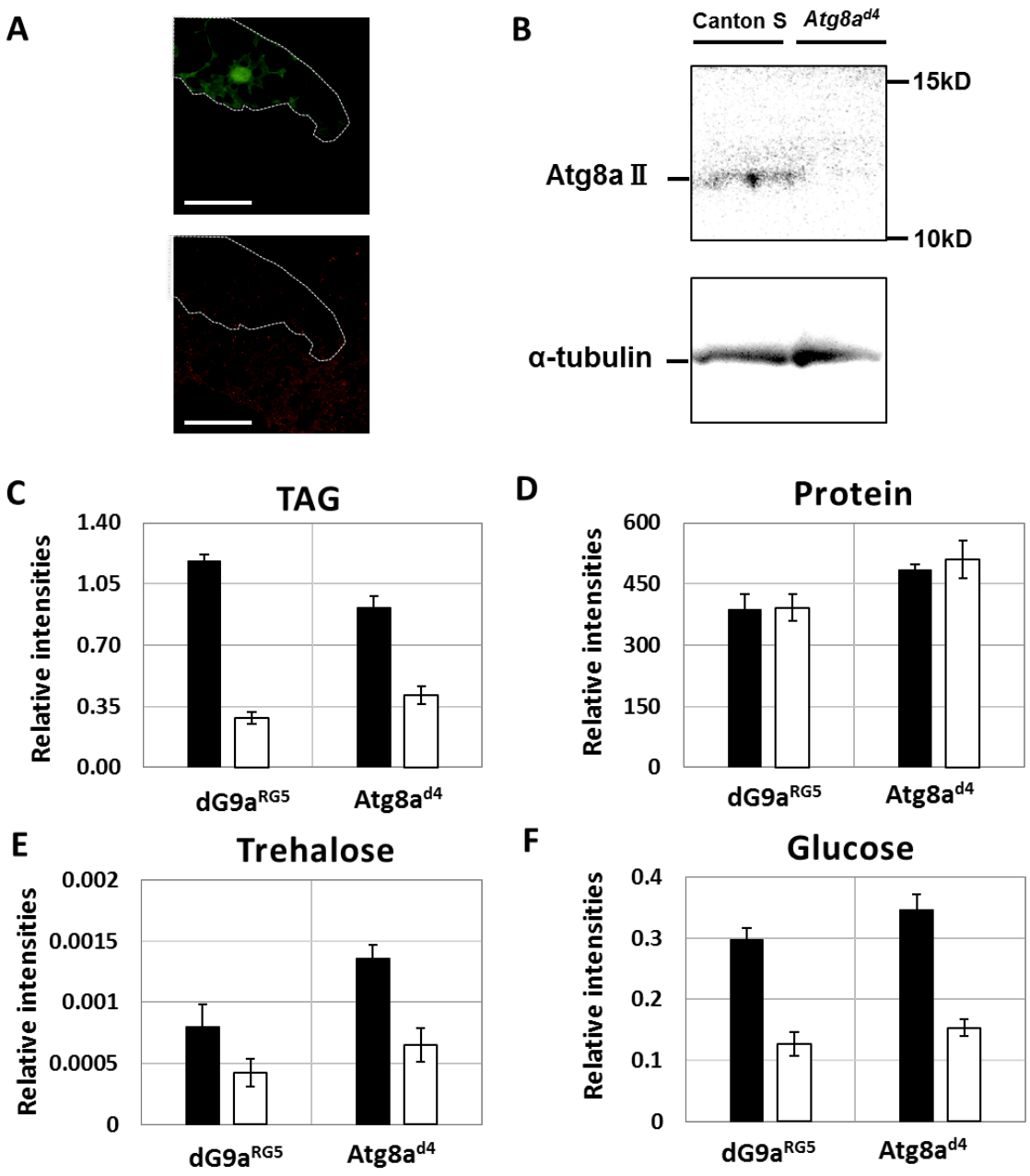

Figure S4. (A) Immunostaining of the larval fat body with anti-Atg8a IgG (α-Atg8a) and anti-GFP IgG (α-GFP). Atg8a down-regulated clones marked by GFP were generated in larval fat body. Scale bars: 50μm. **(B)** A western blot analysis of extracts from Canton S and *Atg8a^{d4}*. Blots were probed with anti-Atg8a and anti-α-tubulin antibodies. The comparison of TAG, total protein, trehalose and glucose levels between *dG9a^{RG5}* and *Atg8a^{d4}* were shown in **(C), (D), (E)** and **(F)**, respectively. No significant differences were observed between *dG9a^{RG5}* and *Atg8a^{d4}* at 24 h after starvation. Error bars represent SE.

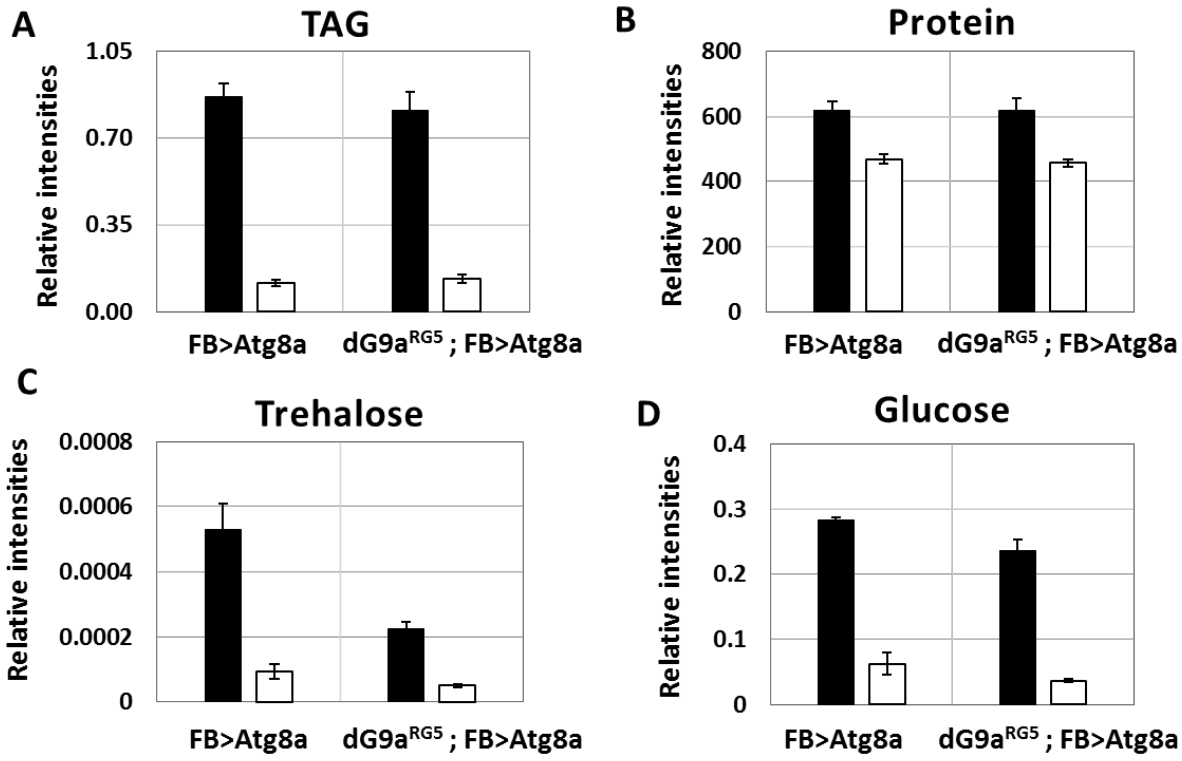

Figure S5. The comparison of energy reservoirs between the males of *dG9a*^{RG5}, FB>Atg8a (*dG9a*^{RG5}*; FB-GAL4/ Atg8a*$^{Scer/UAS.P/T.T:Avic/GFP-EGFP,T:Disc/RFP-mCherry}$*;* +) (n=39 from 2 independent experiments) and FB>Atg8a (+*; FB-GAL4/ Atg8a*$^{Scer/UAS.P/T.T:Avic/GFP-EGFP,T:Disc/RFP-mCherry}$*;* +) (n=38 from 2 independent experiments) strains. The level of TAG, total protein, trehalose and glucose were shown in **(A), (B), (C),** and **(D)**, respectively. No significant differences were observed at 24 h after starvation. Error bars represent SE.

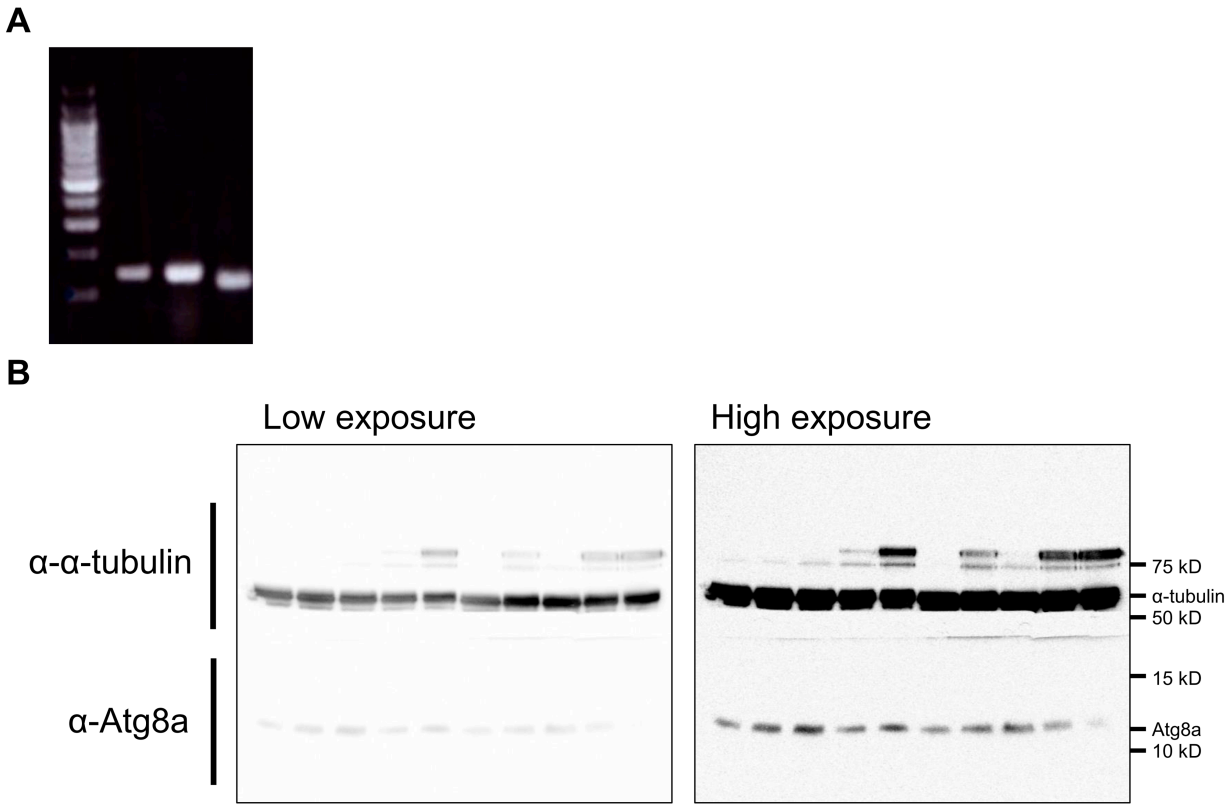

Figure S6. (A) The full-length image of Figure 2F. **(B)** The full-length image of Figure 6B.